

## QUASI-STATIC MECHANICAL BEHAVIOR OF A DOUBLE-SHEAR SINGLE DOWEL WOOD CONNECTION

**Cristóvão L. Santos, clsantos@utad.pt**

**Abílio M.P. De Jesus, ajesus@utad.pt**

Departamento de Engenharias, Universidade de Trás-os-Montes e Alto Douro, Quinta de Prados, 5001-801 Vila Real, Portugal

**José J.L. Morais, jmorais@utad.pt**

CETAV/Departamento de Engenharias, Universidade de Trás-os-Montes e Alto Douro, Quinta de Prados, 5001-801 Vila Real, Portugal

**José L.P.C. Lousada, jlousada@utad.pt**

Departamento de Florestal, Universidade de Trás-os-Montes e Alto Douro, Quinta de Prados, 5001-801 Vila Real, Portugal

**Abstract.** Results of a double-shear single-dowel wood connection tested under monotonic quasi-static tensile loading are presented and discussed in this paper. The wood used in this study was a pine wood, namely the *Pinus pinaster* Ait. species, which is one of the most important Portuguese species. The connection wood members are loaded in the parallel-to-grain direction according to the recommendations of the EN26891 standard. The complete load-slip behavior of the joint is illustrated until failure. In particular, the initial joint slip modulus, the ultimate strength and the ductility are evaluated and compared with corresponding values given by the Eurocode 5. Also, embedding tests are carried out in parallel-to-grain direction, both in compression and tension, according to the EN383 standard. The resulting data is used for predicting the behavior of the wood connection. Finally, a three dimensional finite element model of the wood connection is built using the commercial FEA code, ANSYS®. The dowel is modeled as an isotropic elastic material; the wood is considered as an orthotropic elastic material. The interaction between the dowel and the wood is simulated using contact elements, namely surface-to-surface contact elements available in the ANSYS. The application of contact elements turns nonlinear the analysis, requiring an incremental load stepping. Since the materials are considered as elastic, then it is only expected to model the initial joint slip modulus. Therefore, the initial joint slip modulus is evaluated and compared with the experimental data. Additionally stress fields are illustrated, especially around the dowel.

**Keywords:** Pine wood, dowel-type connection, double-shear, tensile testing, Finite Element Analysis

### 1. INTRODUCTION

The connections are frequently the critical locations of wood structures, being responsible for the reduction of continuity and the global structural strength, requiring oversized structural elements. About 80% of failures observed in wood structures are due to connections (Itany and Faherty, 1984). Dowel-type wood connections are the most common connections applied in wood structures. The singularity of this type of wood connections is associated to the combination of very distinct materials – wood and steel – and to the high anisotropy of wood. The knowledge of the mechanical behavior of these dowel type connections (e.g. load-slip relation, stress distribution, ultimate strength and failure modes) is of primordial importance for their rational application. This complex behavior is governed by several geometric, material and load parameters (e.g. wood species, dowel diameter, end and edge distances, space between connectors, number of connectors, clearance, friction and load configuration).

According to design codes of current practice (Soltis and Wilkinson, 1987) (CEN, 2004), the design of dowel type wood connections has been based on the European Yield Model proposed by Johansen (1945). This model has an empirical basis and assumes an elastic-perfect plastic behavior, for both wood and dowel. It also considers that embedding strength is a material property, when in fact it is a combination of several geometric and material parameters. Generally, in order to verify the influence of those parameters a number of tests are required for assessing the embedding strength. These embedding tests are standardized such as in the EN383 standard (CEN, 1993a).

The Johansen model only predicts ductile failure modes (Patton-Mallory *et al.*, 1997a). Fragile failures observed in single or multiple dowel connections are not envisaged by the Johansen model. Alternative 2D models have been proposed such as nonlinear beam on foundation (Patton-Mallory *et al.*, 1997a) (Sawata and Yasamura, 2003) and finite element (FE) models (Patton-Mallory *et al.*, 1997a) (Chen *et al.*, 2003) (Racher and Bocquet, 2005) (Kharouf *et al.*, 2003). However, it has been recognized that these models only give reasonable predictions for very specific extreme situations such as very thin or very thick wood members. Typically, dowel type connections are three dimensional problems (non-uniform stress distributions across the thickness of members) that must be accounted for a convenient modeling. Few 3D FE models can be found in literature to model the mechanical behavior of single-fastener joints (Patton-Mallory *et al.*, 1997b) (Moses and Prion, 2003). However, no comprehensive FE models for multi-fastener joints are available in literature. Many modeling issues are controversial in the FE models, such as the choice of the appropriate constitutive models for wood and the adequate failure criteria. Also, deterministic approaches are the

common procedure, which represents an important limitation since the problem is governed by several important parameters with stochastic nature (e.g. wood properties, dimensions).

This paper presents results from monotonic quasi-static tensile tests of a double-shear single-dowel wood connection made of pine wood, namely the *Pinus pinaster* Ait. species, which is one of the species with large implantation in Portugal. Despite the abundance of this raw material, its use for structural applications has been disregarded due to several reasons, such as the cultural and lack of data about the behavior of this material. The connection wood members are loaded in the parallel-to-grain direction according to the recommendations of the EN26891 standard (CEN, 1993b). The whole load-slip behavior of the joint is illustrated until failure. In particular, the initial joint slip modulus, the ultimate strength and the ductility are evaluated and compared with corresponding values given by the Eurocode 5. Also, embedding tests are carried out in parallel-to-grain direction, both in compression and tension, according to the EN383 standard. The resulting data is used for predicting the behavior of the wood connection.

Finally, a three dimensional finite element model of the wood connection is built using the commercial Finite Element Analysis code, ANSYS® (SAS, 2005). The dowel is modeled as an isotropic elastic material; the wood is considered as an orthotropic elastic material. The interaction between the dowel and the wood is simulated using contact elements, namely surface-to-surface contact elements available in the ANSYS. The application of contact elements turns nonlinear the analysis, requiring an incremental load stepping. Since the materials are considered as elastic, then it is only expected to model the initial joint slip modulus. Therefore, the initial joint slip modulus is evaluated and compared with the experimental data. Additionally, stress fields are illustrated, especially around the dowel.

## 2. EXPERIMENTAL RESULTS

### 2.1. Experimental details

This paper presents results of an experimental program which includes monotonic quasi-static tensile tests of a double-shear single-dowel wood connection, performed according to the EN383 standard. Also, embedding tests were carried out using single wood members; both tensile and compressive loading were tested as suggested by the EN383 standard. The load direction was parallel-to-grain for all experiments. Figure 1 depicts the tests configurations, including the geometries of the specimens and test rigs. A nominal diameter of the dowel ( $d$ ) equal to 14 mm was selected; the dimensions of the specimens were defined proportionally, according to the standards.

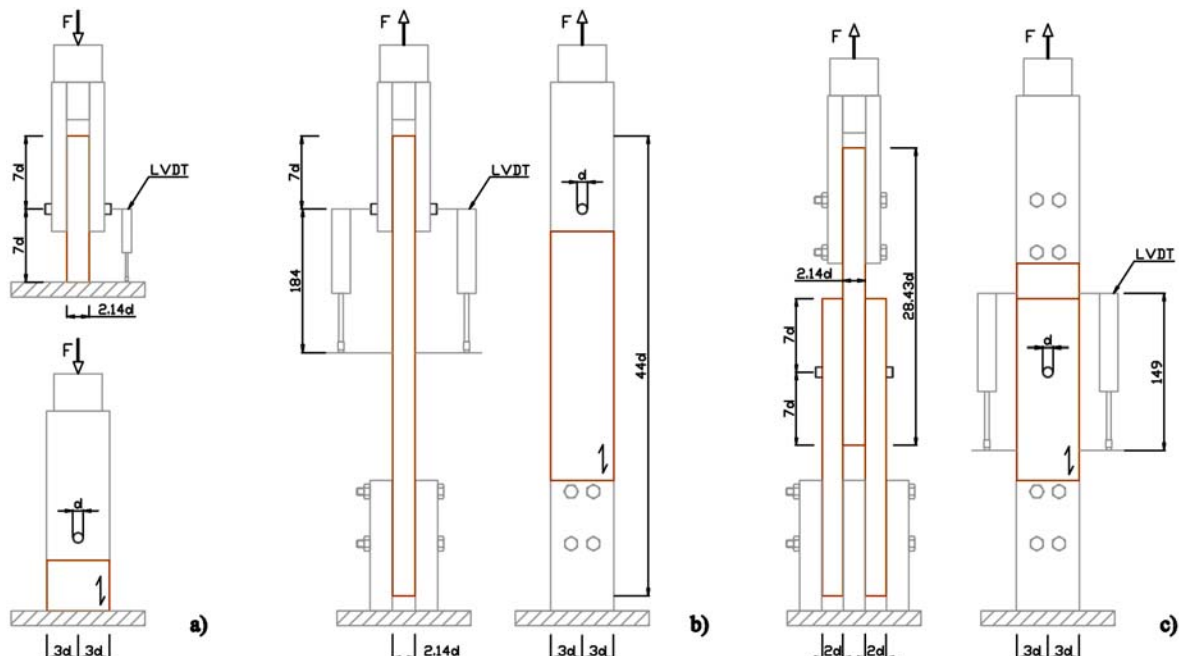


Figure 1. Test configurations: a) parallel-to-grain compression; b) parallel-to-grain tension; c) double shear dowel connection.

The specimens were manufactured using Portuguese pine wood, namely the *Pinus pinaster* Ait. species. All wood required for the experimental program was extracted from selected pine trees. Subsequent cutting and drying processes were fully controlled by authors taking more than one year. The wood was air-dried for a moisture content of about 12%. The specimens were prepared from clear wood matching the wood parallel-to-grain direction with the length of specimens and the wood tangential direction with the thickness of specimens. Table 1 summarizes the experimental

program. Three series were tested specifically longitudinal compression (LC) (see Fig. 1a), longitudinal tension (LT) (see Fig. 1b) and a dowel connection (CON) (see Fig. 1c). Density values were measured based directly on specimens overall volume and respective values are pointed out in Tab. 1. Tests were performed on an INSTRON machine, model 1125, rated to 100 kN. Tests were carried out under crosshead displacement control and were instrumented with LVDT's, model AML/EU  $\pm 10$ -S10 (gauge range of  $\pm 10$  mm), from Applied Measurements®. The experimental data was acquired by a SPIDER 8-30® system.

Table 1. Experimental program.

Series	N.º of specimens	Displacement rate (mm/min)	Density (kg/m <sup>3</sup> )	
			Average	Std. Deviation
LC	24	0.3	570.1	38.3
LT	26	0.5	573.2	49.8
CON	25	0.3	610.7 <sup>(1)</sup>	46.3 <sup>(1)</sup>
			617.8 <sup>(2)</sup>	20.9 <sup>(2)</sup>

<sup>(1)</sup>: central member

<sup>(2)</sup>: complete connection

## 2.2. Results and analysis

Figures 2a and 2b exhibit the load-displacement records from the embedding tests, carried out according to the EN383 standard. The experimental load-slip curves from the connection tests are plotted in Fig. 2c. Both displacement and slip resulted from LVDT's average measurements. Specimens were loaded accordingly the strategy suggested by the EN26891 and EN383 standards, namely they were loaded until 40% of the maximum estimated load ( $F_{est}$ ), and crosshead position held during 30 s. After this stage, specimens are unloaded until  $0.1F_{est}$  and crosshead position again maintained along more 30 s. Finally, specimens are reloaded until failure. Two stiffness values were defined: an initial stiffness,  $k_i$ , determined from linear regression analysis of the load-displacement/slip responses after initial bedding-in displacement/slip and  $0.4F_{est}$ ; a stiffness,  $k$ , determined from a linear regression analysis of the load-displacement/slip response during the unloading/reloading stages. For all tests an ultimate load can be clearly defined.

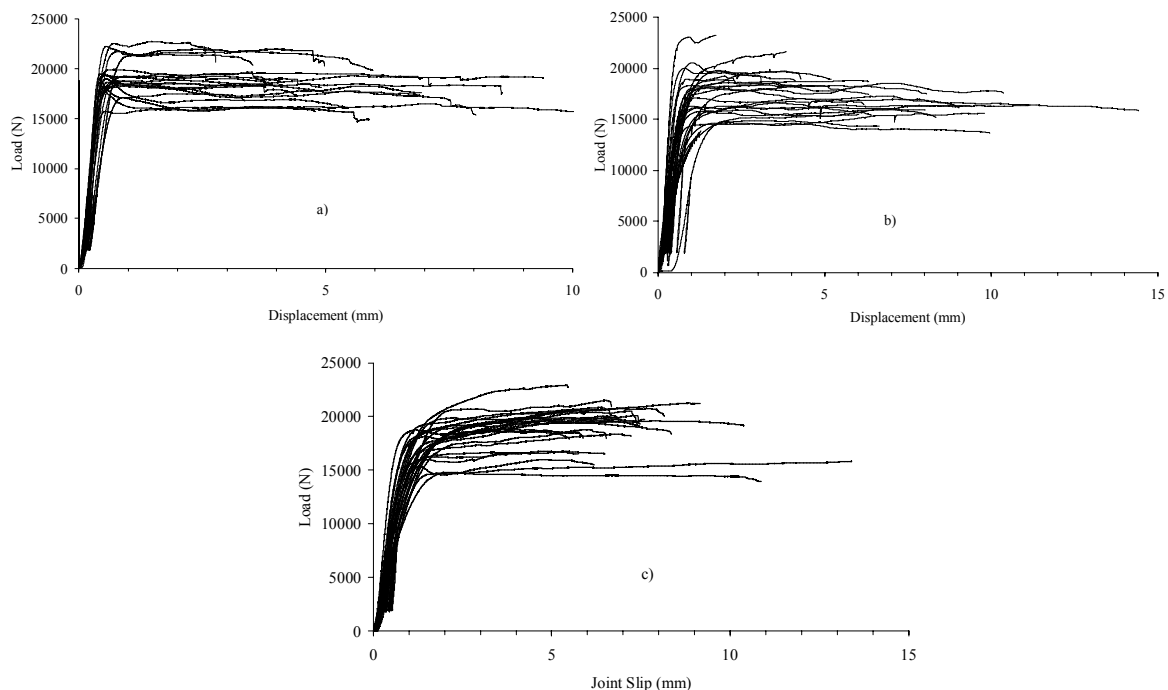


Figure 2. Experimental load-displacement/slip records: a) parallel-to-grain compression; b) parallel-to-grain tension; c) double shear dowel connection.

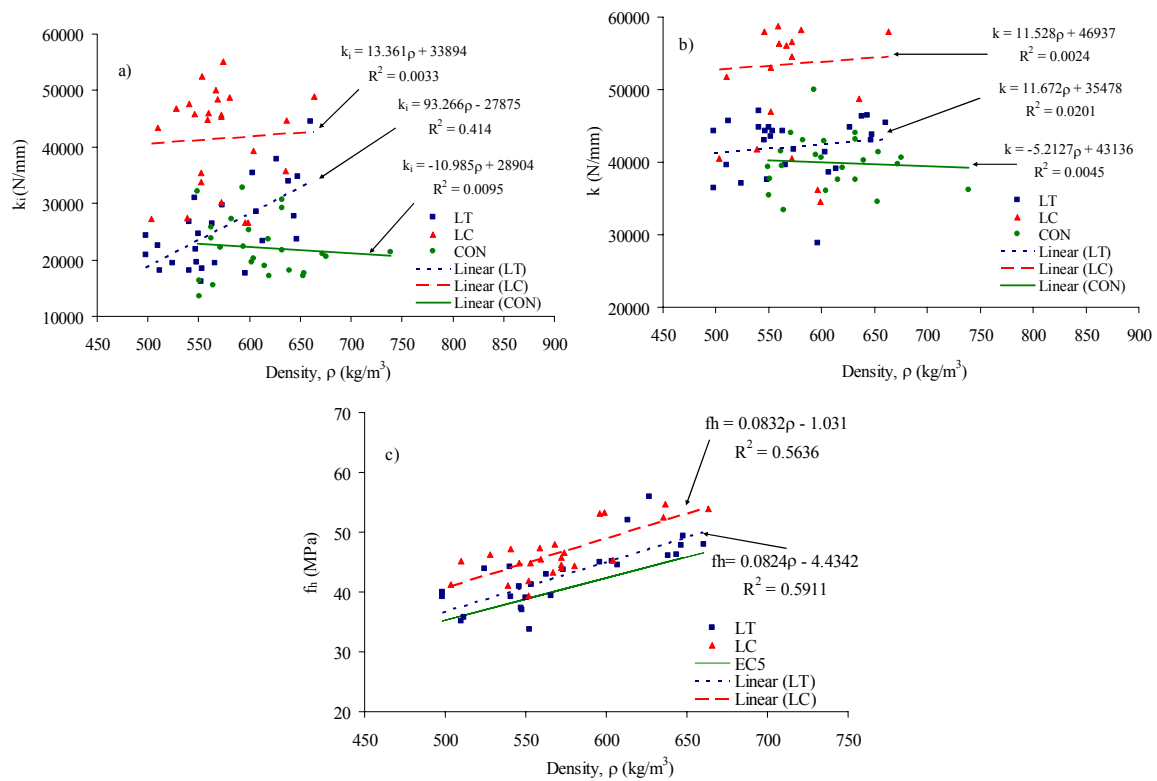


Figure 3. Experimental results: a) initial stiffness; b) stiffness; c) embedding strength.

Figures 3a and 3b exhibit the initial stiffness,  $k_i$ , and stiffness,  $k$ , against the wood density. As can be observed there is no significant correlation between stiffness and density and a high scatter can be seen. Table 2 summarizes the average stiffness values. The initial stiffness is appreciably lower than the stiffness measured for the unloading/reloading stages, being the latter usually called elastic stiffness (CEN, 1993a, 1993b). Clearly the longitudinal compression tests led to higher stiffness than the longitudinal tension and joint tests, which confirms the longitudinal tension tests as the best choice for assessing the joint behavior. The differences between the stiffness values from the longitudinal tension and the joint tests can be, in part, justified by the different member lengths, as illustrated in Fig. 1. The stiffness from the longitudinal tension tests can be used to estimate the joint stiffness using a procedure depicted in Fig. 4. The stiffness of each joint members ( $k(L1)$ ,  $k(L2)$ ) are estimated from the stiffness of the longitudinal tension tests ( $k_{LT}$ ) corrected in order to take into account the differences between lengths. It is assumed that member stiffness is composed by two parts: a local bearing stiffness and a remote member stiffness, being the latter only function of the cross sectional area ( $A$ ), longitudinal Young modulus ( $E$ ) and remote length ( $L-X$ ). Based on dimensions from Fig. 1 and assuming  $E=15.1$  GPa, one derive the following joint stiffness values,  $k_{CON}= 18301.6$  N/mm and  $k_{CON}= 31659.9$  N/mm, respectively for the initial stiffness and stiffness. Comparing these values with the experimental ones, these are about 20% lower, which are rough estimates of the joint stiffness.

Table 2 also indicates the displacement/slip at failure for the three test series, which is a measure of the ductility. A significant scatter is observed as indicates the high standard deviations. The majority of the tests culminated with a fragile failure of shear-splitting type, however, before this failure occur, the test members experienced important deformations. A few specimens did not exhibit a fragile failure. Figure 5 shows the appearance of observed typical failures.

Table 2. Experimental results.

Series	$k_i$ (N/mm)		$k$ (N/mm)		$f_h$ (MPa)		Displacement/slip at failure (mm)	
	Average	Std. Deviation	Average	Std. Deviation	Average	Std. Deviation	Average	Std. Deviation
LC	41510.8	8864.6	53508.5	8919.1	46.4	4.2	6.09	2.05
LT	25586.0	7215.8	42168.7	4101.6	42.8	5.3	6.62	3.16
CON	22196.0	5224.2	39954.7	3663.7	-	-	7.32	1.96

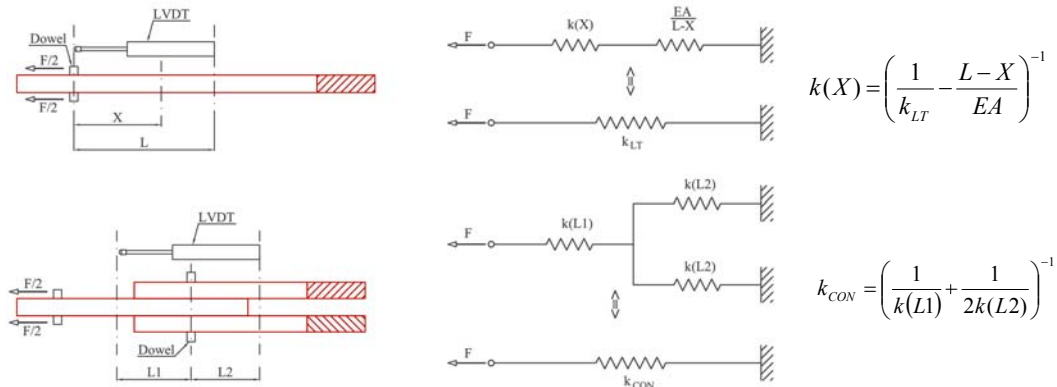


Figure 4. Procedure for joint stiffness estimation.

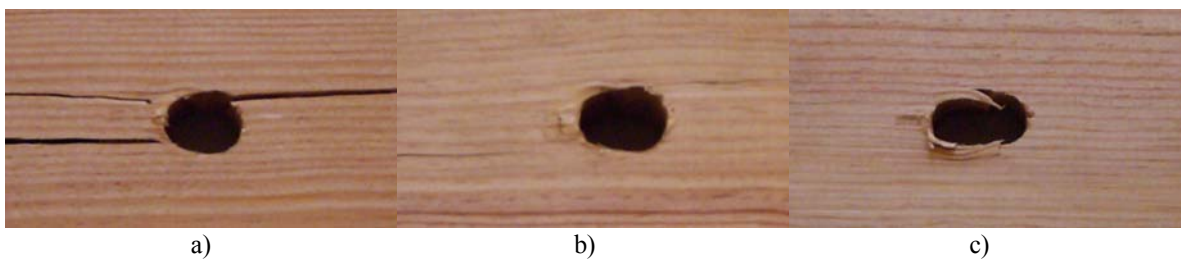


Figure 5. Typical failure modes of the center member of the joint: a) fragile failure – two shear cracks; b) fragile failure – single shear crack and c) ductile failure.

Figure 3c shows the embedding strength data resulted from the tensile and compressive longitudinal tests. A clear correlation between the embedding strength and density can be observed. It is interesting to note that embedding strength from longitudinal compressive tests is greater than the corresponding value from the tensile tests. A comparison between experimental correlations and the Eurocode 5 proposal are also carried out in Fig. 3c. The Eurocode 5 does not distinguish the embedding strength from tension or compression tests; it underestimates both embedding strength values being conservative as would be expected. Both experimental and Eurocode 5 relations show the same trends. Based on the embedding strength relations propose in Fig. 3, the ultimate failure load of the tested joint is evaluated. Both estimations and experimental ultimate failure loads are compared in Fig. 6. The experimental data reveals important scatter around the average trend. Take in to account the average trend the Eurocode 5 still is a safe option. Clearly the longitudinal compression data are not well suited for the joint failure load estimation; the longitudinal tension data seems to be a more appropriate choice, even though the different slopes observed.

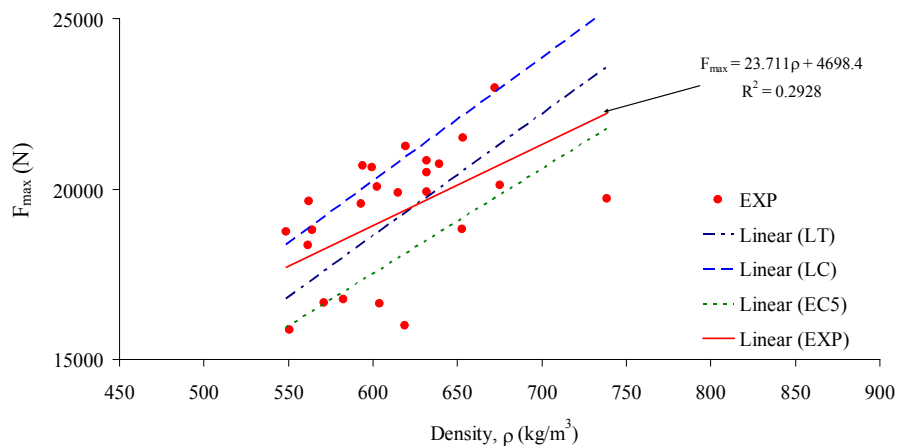


Figure 6. Ultimate load of the tested joint: experimental data and predicts.

### 3. NUMERICAL RESULTS AND ANALISYS

A 3D finite element model of the tested joint was built and results are discussed in this paper. The commercial finite element code, ANSYS 10.0 (SAS, 2005) was used for this purpose. The model was built using the ANSYS parametric design language capabilities – APDL language. Both wood members and steel dowel were accounted in the model. They were modeled using hexahedra isoparametric 20-node elements (SOLID95). The contact between the dowel and wood members was modeled applying the contact elements available in ANSYS, using a surface-to-surface option. In particular, the elements CONTA174 and TARGE170 were used to model respectively the contact and target surfaces, forming the so-called contact pair. Both surfaces in contact were assumed flexible.

Once the joint geometry admits two planes of symmetry, only ¼ of the joint was modeled (½ of a side member and ¼ of the central member). The displacements of the nodes located at the planes of symmetry were restrained in the normal direction to these planes. Three contact pairs were considered, namely one between the dowel and the surface of the hole in side member, another between the dowel and the surface of the hole in central member and finally another contact pair between the surfaces of the side and central wood members. The lengths of the members were assumed equal to the LVDT gauge length as indicated in Fig. 1. Figure 7 shows the finite element mesh built for the joint. The nodes in the base of the side member were restrained in the vertical direction (y) and nodes in the top of the center member were displaced by a maximum value,  $d_{max}=0.1$  mm, in vertical direction.

Both materials were modeled as homogeneous and elastic. While steel was considered isotropic, wood was assumed orthotropic. The elastic properties of the two materials are summarized in Tab. 3. The properties of the wood were identified by Xavier (2003), Oliveira (2003) and Pereira (2003). These properties were derived for wood extracted from trees of same region as those used to extract the wood required for this work. Some preliminary tests, namely tensile and compression tests of small prismatic clear wood specimens, confirmed the properties of Tab. 3.

Assuming linear elastic behaviors for materials is a first step in the simulations, since the model is not able to simulate the nonlinear behavior of the joint including the failure. This model is used in this paper to simulate the joint elastic stiffness, which can be compared with the available experimental results. In spite of assuming elastic materials, the global problem is nonlinear due to the contact. Therefore, an incremental loading is applied – the maximum displacement of 1 mm was applied in 10 equal increments.

The contact problem is governed by an important number of parameters, such as the contact algorithm, friction model, normal contact stiffness, tangential contact stiffness, maximum penetration, etc. Also, each contact pair requires the definition of the contact and target surfaces that will be meshed with CONTA174 and TARGE170 elements, respectively. Furthermore to the contact model parameters, geometric parameters can also play an important role on contact behavior, such as the dowel-hole gap.

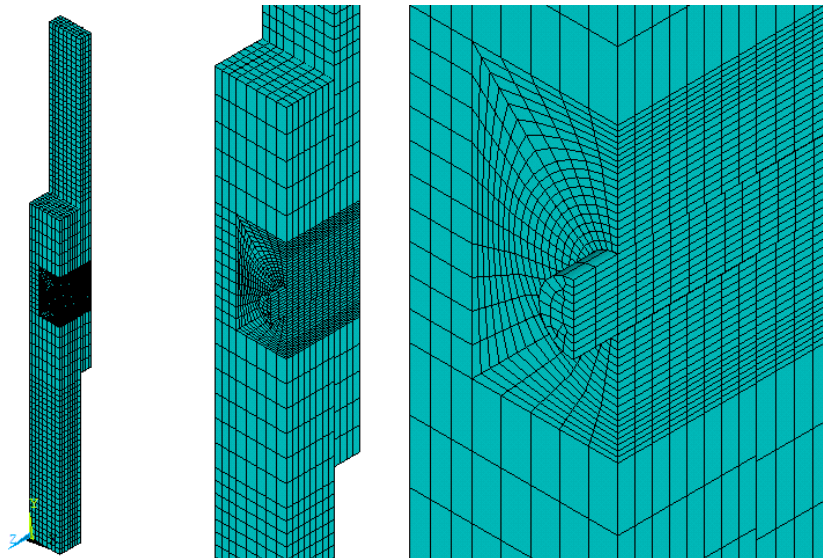


Figure 7. Finite element mesh of the double-shear single dowel joint.

Table 3. Elastic material properties.

	E [GPa]	$\nu$	$E_L$ [GPa]	$E_R$ [GPa]	$E_T$ [GPa]	$\nu_{LR}$	$\nu_{RT}$	$\nu_{TL}$	$G_{LR}$ [GPa]	$G_{LT}$ [GPa]	$G_{RT}$ [GPa]
Dowel steel	210	0.27									
Wood			15.13	1.91	1.01	0.47	0.59	0.05	1.35	1.51	0.25

Simulations were carried out using the augmented Lagrange algorithm available in the ANSYS (SAS, 2005). Since the contact pair behavior is governed by several parameters a set of 24 simulations were carried out in order to better understand the influence of some of those parameters on joint behavior, especially on stiffness. For the contact pair between the two wood members, default ANSYS (version 10.0) parameters were used since it is expected that this interface behavior will not govern the global joint behavior. For the other two contact pairs other parameters were used, but using the same values for both. All simulations were carried out assuming the Coulomb friction model, for two distinct friction coefficients:  $\mu=0.0$  (12 simulations) and  $\mu=0.5$  (12 simulations). The augmented Lagrangian method requires the definition of normal and tangential contact stiffnesses. The amount of penetration between contact and target surfaces depends on the normal stiffness. Higher stiffness values decrease the amount of penetration, but can lead to ill-conditioning of the global stiffness matrix and to convergence difficulties. Lower stiffness values can lead to a certain amount of penetration and produce an inaccurate solution. Ideally, you want a high enough stiffness that the penetration is acceptably small, but a low enough stiffness that the problem will be well-behaved in terms of convergence.

Table 4. Model configurations and numerical results.

SIMULATIONS					RESULTS						
Config.	GAP (mm)	FKN	FTOLN	$\mu$	N.º Iterations	k (N/mm)	Stress, $\sigma_y$ (MPa)		Max. contact values		
							Max	Min	Penetr. (mm)	Pressure (MPa)	Sliding (mm)
01	0.1	0.1	0.10	0.0	20	31407.0	11.3	-18.1	0.014921	5.422	0.012178
02	0.1	1.0	0.10	0.0	20	46117.0	14.8	-21.4	0.002667	7.046	0.016396
03	0.1	0.1	0.05	0.0	20	31407.0	11.3	-18.1	0.014921	5.422	0.012178
04	0.1	1.0	0.05	0.0	20	46117.0	14.8	-21.4	0.002667	7.046	0.016396
05	0.1	0.1	0.01	0.0	29	37475.0	12.9	-18.6	0.007306	6.652	0.014195
06	0.1	1.0	0.01	0.0	20	46117.0	14.8	-21.4	0.002667	7.046	0.016396
07	0.3	0.1	0.10	0.0	20	25273.0	9.1	-20.0	0.017231	6.421	0.009645
08	0.3	1.0	0.10	0.0	22	39823.0	12.8	-25.7	0.003265	8.996	0.015404
09	0.3	0.1	0.05	0.0	20	25273.0	9.1	-20.0	0.017231	6.421	0.009645
10	0.3	1.0	0.05	0.0	23	39823.0	12.8	-25.7	0.003265	8.996	0.015404
11	0.3	0.1	0.01	0.0	30	33964.0	11.2	-22.4	0.007612	7.842	0.014067
12	0.3	1.0	0.01	0.0	23	39823.0	12.8	-25.7	0.003265	8.996	0.015404
13	0.1	0.1	0.10	0.5	27	31420.0	11.2	-17.7	0.015192	5.195	0.010820
14	0.1	1.0	0.10	0.5	22	46499.0	14.9	-21.1	0.002643	6.749	0.005147
15	0.1	0.1	0.05	0.5	27	31420.0	11.2	-17.7	0.015192	5.195	0.010820
16	0.1	1.0	0.05	0.5	22	46499.0	14.9	-21.1	0.002643	6.749	0.005147
17	0.1	0.1	0.01	0.5	36	37610.0	12.8	-17.9	0.007555	6.593	0.007248
18	0.1	1.0	0.01	0.5	22	46499.0	14.9	-21.1	0.002643	6.749	0.005147
19	0.3	0.1	0.10	0.5	27	25254.0	9.0	-19.6	0.017435	6.376	0.005981
20	0.3	1.0	0.10	0.5	29	39901.0	12.7	-26.3	0.003345	9.000	0.003030
21	0.3	0.1	0.05	0.5	27	25254.0	9.0	-19.6	0.017435	6.376	0.005981
22	0.3	1.0	0.05	0.5	29	39901.0	12.7	-26.3	0.003345	9.000	0.003030
23	0.3	0.1	0.01	0.5	35	33902.0	11.1	-22.7	0.007738	7.804	0.004169
24	0.3	1.0	0.01	0.5	29	39901.0	12.7	-26.3	0.003345	9.000	0.003030

ANSYS provides default values for contact stiffness which can be scaled by user through the FKN parameter. The usual factor range is from 0.01-1.0, with a default of 1.0. The default value is appropriate for bulk deformation. Present simulations covered FKN values equal to 0.1 and 1.0. Another relevant contact parameter to be used in conjunction with the augmented Lagrangian method is FTOLN. FTOLN is a tolerance factor to be applied in the direction of the surface normal. The range for this factor is less than 1.0 (usually less than 0.2), with a default of 0.1, and is based on the depth of the underlying solid element. This factor is used to determine if penetration compatibility is satisfied. Contact compatibility is satisfied if penetration is within an allowable tolerance (FTOLN times the depth of underlying elements). The depth is defined by the average depth of each individual contact element in the pair. If ANSYS detects any penetration larger than this tolerance, the global solution is still considered unconverged, even though the residual forces and displacement increments have met convergence criteria. FTOLN values equal to 0.01, 0.05 and 0.1 were simulated. For all other contact parameters not mentioned here default values were adopted (SAS,2005).

The contact performance is strongly influenced by the gap between dowel and hole. The geometric parameter is not easy to estimate due to the difficulty on dimensional control of manufactured holes. Also, a bedding-in phenomenon is observed between the dowel and the hole, which eliminates any irregular surface roughness and misalignments, contributing, in practice, to increase this gap. Based on direct measurements and on the unloading branch of the load slip curves, we concluded that gaps in the range of 0.1-0.3 mm are realistic. Thus, simulations were carried out considering the two extreme gap values of the referred range.

Table 4 summarizes the configurations of the simulations and respective numerical results. Results include the joint stiffness (slip modulus), the maximum and minimum stresses on the surface of the holes and some relevant contact results, such as the maximum penetration, pressure and sliding. Also, the number of iterations is included in the table, since it serves as a measure of the computational cost, which is important for nonlinear simulations.

The joint stiffness is the only numerical result that can be assessed using the available experimental data, namely the joint stiffness obtained at the unloading-reloading stages (see Tab. 2). The experimental average stiffness falls within the range of numerical results. The gap has a determinant effect on stiffness values; its increase results in a systematic stiffness reduction. For frictionless contact and using default values of FKN and FTOLN with GAP=0.3 (configuration 08), simulations yield about the same value of the average experimental stiffness. Considering friction coefficient of 0.5 (configuration 20) this stiffness slightly increases getting even better. Consideration of a non-null friction coefficient yields a slightly results change, with an increase in computational cost, since the stiffness matrix of the structure become unsymmetric.

The FKN factor also plays an important role on contact simulation as demonstrated by the numerical results of Tab. 4. In fact, the reduction of this factor produces a significant reduction on the joint stiffness. Apparently the FTOLN parameter has a minor influence on results; only for small values of this parameter, changes in results are visible since more iterations are needed to accommodate a smaller penetration. In all simulations the numerical penetration was kept very small as certified the maximum penetration value of Tab. 4 (17  $\mu\text{m}$ ).

Figure 8 illustrates the stress field acting in parallel-to-grain direction for the configuration 20. It is clear that the extreme values are observed around the dowel and the through thickness stress distribution is not uniform. The maximum compressive stress is verified in the inner wood member, which is consistent with the experimental tests. In fact the failure occurred always in the inner member – the most stressed one. Figure 9 shows some contact results, in particular the contact penetration, pressure and sliding distance, again for the configuration 20.

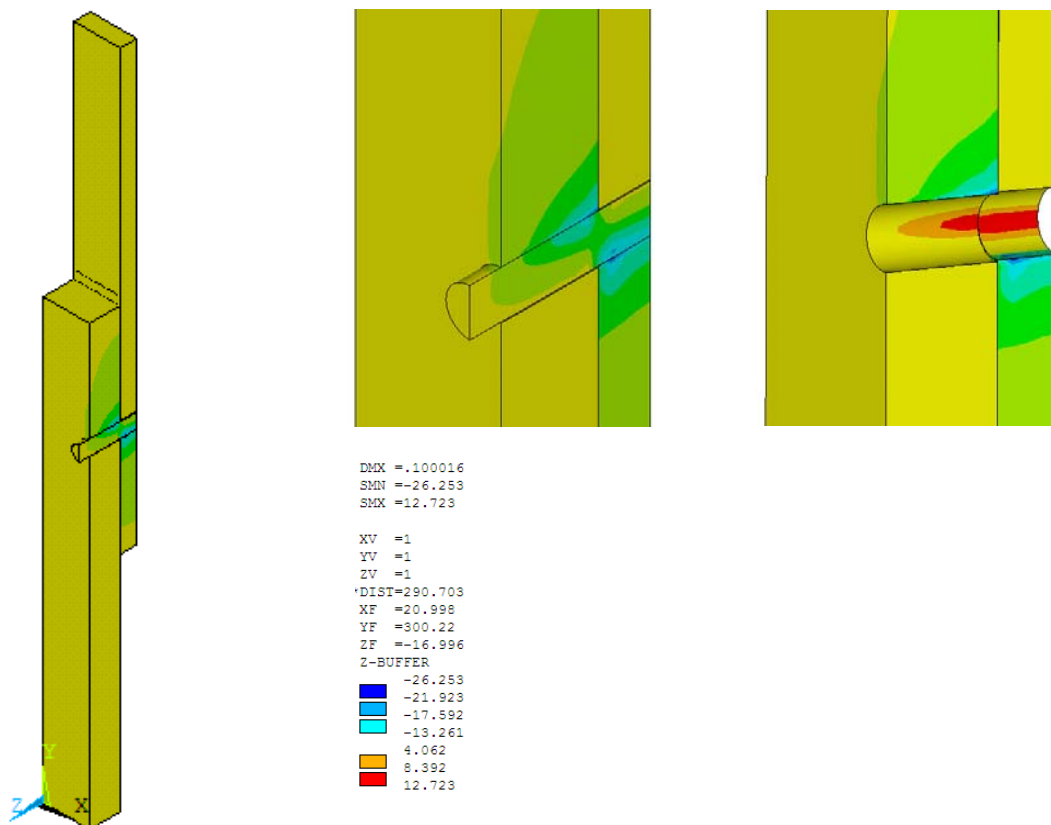


Figure 8.  $\sigma_y$  stresses in MPa, obtained with configuration 20.



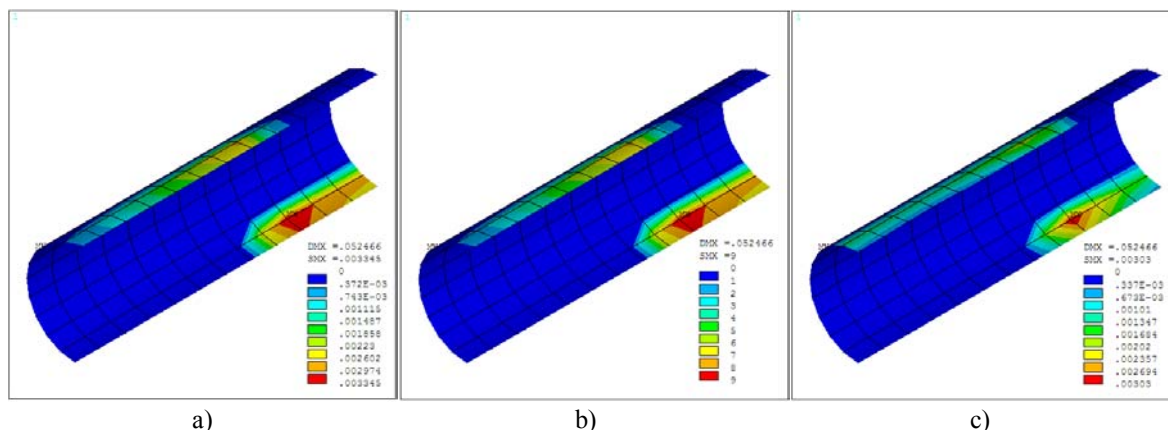


Figure 9. Contact values obtained with configuration 20: a) penetration in mm; b) pressure in MPa and c) sliding distance in mm.

#### 4. CONCLUDING REMARKS

This paper reported both experimental and numerical work about the mechanical behavior of a double-shear single dowel wood connection made of Portuguese pine wood. The experimental work also included embedding tests of the in order to evaluate strength data required for the joint analysis. As far as the authors are aware there are available in literature very few data about the Portuguese pine wood, which makes this work relevant. Also, there are only few 3D finite element models for wood connections available in literature, which makes this paper even more relevant, since a finite element model is proposed and discussed.

In what concerns the experimental results, it was demonstrated that the tensile embedding tests are the best option to derive data for accessing the joint.

The simulations were able to accurately estimate the joint stiffness using the contact technology and defaults from ANSYS encouraging the next step in simulations: to include material nonlinearities.

#### 5. ACKNOWLEDGEMENTS

The authors wish to express their gratitude to the graduation students, Vitor Costeira and Ricardo Leal, for their collaboration in some experimental and numerical tasks, and also to Sr. Armindo Teixeira for his contribute on specimens preparation.

#### 6. REFERENCES

- European Committee for Standardization, 2004, EN 1995-1-1 Design of timber structures. Part 1-1: General rules and rules for buildings, Brussels.
- European Committee for Standardization, 1993a, EN383: Timber Structures. Test Methods. Determination of embedding strength and foundation values for dowel type fasteners, European Standard.
- European Committee for Standardization, 1993b, EN26891: Timber Structures. Test Methods. Determination of embedding strength and foundation values for dowel type fasteners, European Standard.
- Chen, C.J., Lee, T.L. and Jeng, D.S., 2003, "Finite element modelling for the mechanical behaviour of dowel-type timber joints," *Computers and Structures*, Vol. 81, pp. 2731-2738.
- Itany, R.Y. and Faherty, K.F., 1984, *Structural wood research, state-of-the-art and research needs*, ASCE, New York.
- Kharouf, N., McClure, G. and Smith, I., 2003, "Elasto-plastic modelling of wood bolted connections", *Computers and Structures*, Vol. 81, pp. 747-754.
- Moses, D.M.; Prion, H.G.L., 2003, "A three-dimensional model for bolted connections in wood", *Canadian Journal of Civil Engineering*, Vol. 30, pp. 555-567.
- Oliveira, M., 2003, *Caracterização do comportamento ao corte da madeira usando o ensaio de Arcan*, Tese de Mestrado, Universidade de Trás-os-Montes e Alto Douro, Vila Real.
- Patton-Mallory, M. Cramer, S.M., Smith, F.W. and Pellicane, P.J., 1997b, "Nonlinear material models for analysis of bolted wood connections", *Journal of Structural Engineering*, Vol. 123, No. 8, pp. 1063-1070.
- Patton-Mallory, M., Pellicane, P.J. and Smith, F.W., 1997a, "Modelling bolted connections in wood: review", *Journal of Structural Engineering*, Vol. 123, No. 8, pp. 1054-1062.
- Pereira, J., 2003, *Comportamento mecânico da madeira em tracção nas direcções de simetria material*, Tese de Mestrado, Universidade de Trás-os-Montes e Alto Douro, Vila Real.

- Racher, P.; Bocquet, J.F., 2005, “Non-linear analysis of dowelled timber connections: a new approach for embedding modelling”, *Electronic Journal of Structural Engineering*, Vol. 5, pp. 1-9.
- Sawata, K.; Yasamura, M., 2003, “Estimation of Yield and Ultimate strengths of bolted timber joints by nonlinear analysis and yield theory”, *Journal of Wood Science*, Vol. 49, pp. 383-391.
- Soltis, L.A. and Wilkinson, T.L., 1987, *Bolted-Connection Design*, General Technical Report FPL-GTR-54, Forest Products Laboratory – USDA, Madison, WI.
- Swanson Analysis Systems Inc., 2005, *ANSYS*, Version 10.0, Houston.
- Xavier, J.C., 2003, *Caracterização do comportamento ao corte da madeira usando o ensaio de Iosipescu*, Universidade de Trás-os-Montes e Alto Douro, Vila Real.

## **7. RESPONSIBILITY NOTICE**

The authors are the only responsible for the printed material included in this paper.